A Shock-Refracted Acoustic Wave Model for the Prediction of Screech Amplitude in Supersonic Jets

M. Kandula

Sierra Lobo Inc. (USTDC), John F. Kennedy Space Center, FL, USA

A physical model is proposed for the estimation of the screech amplitude in underexpanded supersonic jets. The model is based on the hypothesis that the interaction of a plane acoustic wave with stationary shock waves provides amplification of the transmitted acoustic wave upon traversing the shock. Powell's discrete source model for screech incorporating a stationary array of acoustic monopoles is extended to accommodate variable source strength. The proposed model reveals that the acoustic sources are of increasing strength with downstream distance. It is shown that the screech amplitude increases with the fully expanded jet Mach number. Comparisons of predicted screech amplitude with available test data show satisfactory agreement. The effect of variable source strength on directivity of the fundamental (first harmonic, lowest frequency mode) and the second harmonic (overtone) is found to be unimportant with regard to the principal lobe (main or major lobe) of considerable relative strength, and is appreciable only in the secondary or minor lobes (of relatively weaker strength).

INTRODUCTION

Supersonic jet screech constitutes an important technological challenge in the theory of jet noise. Screech refers to high-amplitude discrete tones superposed on the otherwise broadband acoustic spectrum observed in imperfectly expanded supersonic jets (Fig. 1). The shock noise produced by imperfectly expanded (choked) jets is very complex, and consists of two separate components, namely broadband shock noise (arising from shock-turbulence interaction) and screech tones. This shock noise is in addition to the broadband turbulent mixing noise in the jet (Lighthill 1952, 1954; Ffowcs Williams 1963). In the nearfield, the very high intensity of these screech tones (as high as 170 to 180 dB) with a highly directional character with significant upstream propagating component can induce fatigue and cause serious structural damage and failure of aerodynamic vehicles in flight. A fundamental understanding of jet screech amplitude is thus requisite to the design of a new generation of rocket engines (Kandula 2006a,b), turbo-jet aircraft engines, and to a number of other flow circumstances such as jet impingement and cavity resonance involving feedback cycles.

Owing to pressure mismatch (nozzle exit pressure exceeds the ambient pressure), underexpanded supersonic jet structures manifest themselves in shock-cell structures involving normal/oblique shocks and regions of expansion (Fig. 2). Under certain conditions, a Mach disc is also formed. These shock-expansion units interact with instability waves, vortices, turbulence, and other stream disturbances in the viscous shear layer that surrounds the inviscid region.

Powell (1953a-c) first identified the mechanism of supersonic jet screech in terms of a resonant feedback loop or cycle that is self-sustaining and consists of the following key processes (Fig. 2): downstream passage of flow disturbances in the jet shear layer initiated near the nozzle lip region (where the relatively thin shear layer is susceptible to instability); interaction of these stream disturbances with the nearly periodic and stationary oblique shock-cell structure of the jet resulting in their amplification, with the ultimate generation and emission of intense acoustic waves or energy; upstream propagation of the acoustic waves immediately outside the jet shear layer (acoustic feedback); excitation and maintenance of stream disturbances in the vicinity of the nozzle lip by the upstream propagating acoustic waves (so-called receptivity), which then propagate downstream, thus closing the feedback cycle without any external interference. Experimental data (for example, flow visualization measurements by Kaji & Nishijima 1996) suggest that the shock-noise is most intense somewhere between the third and fourth shock-cell structures. For a detailed discussion on screech, Seiner (1984) may be consulted.

Powell's theory of stationary array of discrete monopole sources distributed through the shock-cells (Powell 1953a) provided directivity patterns of screech that agree with measurements, as reported by Norum (1983) for unheated jets. It also furnished a framework for the estimation of screech frequency based on shock-cell spacing. Fisher & Morfey (1976) and Tam et al. (1986) provided expressions for the prediction of screech frequency over a wide range of fully expanded jet Mach number M_j and jet total temperature T_0. Tam's expression for the screech is predicated on the so-called weakest-link theory, according to which the feedback acoustic waves represent the weakest link and control the screech frequency. Recently, Massey & Ahuja (1997) expanded on Tam's formulation and provided expressions for screech frequency for hot jets with different screech modes. The screech mode changes from axisymmetric to helical and flapping modes as the Mach number M_j increases.

On the basis of Powell's model of stationary point sources, Harper-Bourne and Fisher (1973) experimentally and theoretically treated broadband shock noise (radiated to the farfield) by considering shock-turbulence interaction. Harper-Bourne and Fisher considered spatial coherence of the disturbance field to account for the broadband sound radiation to the farfield. Generally speaking, the intensity of broadband shock-associated noise is more prevalent in the forward arc, and is a function only of the pressure ratio. A stochastic model for broadband shock noise was reported by Tam (1987) who considered the nonlinear interaction between jet turbulence and stationary shock-cell system. Shock-turbulence interaction (shear layer and an oblique compression wave) was numerically investigated by Lui & Lele (2002) including the dynamic motion of the shock during interaction with shear layer vortices.

With regard to the screech process, our current understanding of the highly nonlinear flow dynamics and of the rate of amplification of stream disturbances is rather incomplete. Whereas screech frequency is controlled by the feedback acoustic waves, the screech intensity is governed primarily by the characteristics of the downstream propagating flow disturbances and their interaction with the shock-cell structures. Several detailed measurements (Kaji & Nishijima 1996; Norum 1982; Panda et al. 1997; Panda 1998, 1999; Massey et al. 1993; Krothapalli et al. 1986; Petitjean 2005) and numerical viscous simulations (Kaji & Nishijima 1996; Shen & Tam 2002; Manning & Lele 1998, 2002; Loh et al. 2003; Li & Gao 2004, 2005) have been reported and served to throw light on the subject. The experimental description of A-D mode switch (A_1, A_2, B, C, D; Norum 1982) according to the jet operating parameters represents a notable step. Despite the theoretical advances in screech frequency predictions, directivity character, modulations of instability waves by shocks (Glaznev 1973; Sedel'nikhov 1967) and unsteady shock motions and their role in noise generation, screech amplitude predictions remain elusive (1998, 1999). Owing to strong nonlinearity of the feedback loop, even an empirical formula for screech intensity is unavailable (Shen & Tam 2002).

The preponderating questions concerning the interaction of shock waves with stream disturbances and the excitation of disturbances by upstream-traveling acoustic waves largely remain unanswered. The purpose of the present report is to investigate the amplitude of screech based on a physical model for the interaction of stream disturbances (primarily regarded as finite-amplitude acoustic waves) with shock waves. This paper is primarily based on the author's recent work (Kandula 2006c).

I. PROPOSED PHYSICAL MODEL

A. Source Distribution

The present model builds on Powell's conception of stationary discrete acoustic monopoles (Fig. 3). However, in the present context account is taken of the variable strength of the monopoles, as the flow disturbances are amplified on their passage through the shock-cell system. As with Harper-Bourne and Fisher (1973) the acoustic sources are regarded to be distributed along the lip line at locations in the jet shear layer where shock reflections take place. It is assumed that the sources S_1, S_2, S_3 are equally spaced. It is also assumed that relative to the source S_2, the source S_1 leads in phase τ and S_3 lags in an equal amount of phase τ.

The downstream-propagating stream disturbances near the supersonic side of the shear layer and the upstream-traveling acoustic disturbances on the subsonic outer edge of the shear layer form two key components of the feedback process. Attention is focused here on the amplification of downstream-traveling stream disturbances.

B. Shock-Acoustic Wave Interaction

1. Transmission of an Acoustic Wave Through a Normal Shock

The proposed model for the screech amplitude is based on the doctrine that the downstream-propagating stream disturbances in the screech cycle are regarded as acoustic-like (nearly isentropic pressure fluctuations) and are of finite amplitude. The amplification of these disturbances during their passage is a consequence of the interaction between an acoustic wave (of finite amplitude) and a stationary shock wave. If the screech cycle is regarded as analogous to a thermodynamic cycle (with energy transfers occasioned during shock interaction and scattering at the nozzle lip), the acoustic waves form the working medium for the screech cycle. Thus, it is likely that the upstream-propagating acoustic waves and downstream-traveling acoustic waves constitute the screech cycle. The scattering of upstream-propagating acoustic waves by the nozzle lip ensures that this is so, even though some of the incoming acoustic energy is transmitted to the hydrodynamic disturbances or instability waves in the shear layer in the receptivity process.

Unsteady phase-averaged measurements of nearfield pressure fluctuations in a round jet at M_j =1.19 by Panda (1996) indeed reveal that the downstream-propagating disturbances contain both hydrodynamic pulsations and acoustic waves, whereas upstream-propagating components are only acoustic (Raman 1999).

When an acoustic wave (traversing with sound speed relative to the moving fluid) is incident upon the shock from ahead of it (Fig. 4), no reflected acoustic wave can arise because the flow ahead is supersonic, and the acoustic wave (longitudinal isentropic sound wave) is transmitted (refracted) downstream of the shock. At the same time, perturbations in entropy and vorticity (both are nonisentropic and nonacoustic; these isobaric, transverse waves are termed entropy-vorticity waves after Carrier) are generated, which are transported along with the flow behind the shock (Mckenzie & Westphal 1968; Kontorovich 1960). On the other hand, when an acoustic wave is incident upon the shock from behind it, no disturbances can arise in the medium ahead of the shock. The acoustic waves are merely reflected, and the entropy and vorticity waves are generated behind the shock. Thus, the refraction of the incident acoustic wave is assumed as long as the approach flow is supersonic.

The main relationships developed here are based on transmission through normal shocks, although the shocks in the jet are not wholly normal but oblique. The Mach number normal to the shock M_{1n} is related to the approach Mach number M_1 by the relation

$$M_{1n} = M_1 \sin \beta_1$$

where β_1 represents the shock wave angle (angle between the approach velocity and the plane of the shock). However, it is believed that the relationships based on the normal-shock assumption provide an upper limit to the screech tone intensity.

The passage and linear interaction of plane disturbances (sound waves) with a shock wave upon normal incidence for an ideal gas was first treated by Blokhitsev (1945) and Burgers (1946). When the perturbing waves are normally incident upon the shock, the transmission coefficient is expressed by Blokhitsev (1945) and Burgers (1946) as

$$\frac{\delta p_2}{\delta p_1} = \frac{2M_{1n}^4 + 2(\gamma+1)M_{1n}^3 + (3\gamma-1)M_{1n}^2 + 1 - \gamma}{(\gamma+1)(1 + M_{1n}^2 + 2M_{2n}M_{1n}^2)} \tag{1a}$$

where δp_1 and δp_2 denote the strength of the incident and refracted acoustic waves, respectively, M_{1n} the normal Mach number of the flow upstream of the shock, M_{2n} the normal Mach number of the flow downstream of the shock, and γ the specific heat ratio. The downstream Mach number is obtained from the Rankine-Hugonoit normal shock relation (Shapiro 1953)

$$M_{2n}^2 = \frac{M_{1n}^2 + 2/(\gamma-1)}{[2\gamma/(\gamma-1)]M_{1n}^2 - 1} \tag{1b}$$

Fig. 5 presents the variation of the pressure amplification $\delta p_2 / \delta p_1$ as a function of incoming Mach number M_1. The pressure amplification is seen to rapidly grow as the upstream Mach number is increased. For large values of M_1, the pressure ratio varies as M_1^2. For oblique shocks ($\beta < 90\,\text{deg}$), the pressure amplification is less than that for the normal shock.

The result of the linear shock-acoustic wave interaction theory has been shown to be in close agreement with the numerical nonlinear Euler simulations by Zang et a. (1984) for incident angles within about 30 deg of the critical angle (zero degree incident angle refers to normal incidence) for the acoustic as well as vorticity wave. Although linear theory is employed here shock-acoustic wave interaction, the successive amplification is considered nonlinear.

2. Successive Amplification (Shock-Cell Interaction)

Based on the general behavior of the Mach number decay for typical underexpanded jet conditions, the following distribution of the approach (or upstream) Mach number for each tip of the shock-expansion unit (shock-cell reflection occurring in the shear layer) may be considered as a rough approximation:

$$M_{1i} = M_r - \left(M_r - 1/\sin\beta_1\right)(i-1)/(m-1) \qquad i = 1,2,\ldots m \tag{2a}$$

where M_r is the upstream Mach number for the first shock-cell, M_{1i} the incident Mach number in the ith shock-cell, and m the total number of active shock-cells under consideration. Thus, Eq. (2a) ensures that $M_{1i} \approx M_r$ for the first shock-cell ($i = 1$), and $M_{1i} = 1/\sin\beta_1$ for the last cell ($i = m$). Based on the available data, the quantity M_r is approximated as

$$M_r \approx 1.4 M_j \tag{2b}$$

The quantity M_{1i} could be more accurately obtained by a direct calculation, using numerical methods. In the present work, the choice of Eq. (2a) for approximating M_{1i} is based on the consideration that it facilitates a simpler formulation of the model.

The fully expanded Mach number M_j is related to the pressure ratio p_t / p_a and the pressure ratio parameter β by

$$M_j = \frac{2}{\gamma - 1}\left[\left(\frac{p_t}{p_a}\right)^{(\gamma-1)/\gamma} - 1\right] \tag{2c}$$

and

$$\beta = \sqrt{M_j^2 - 1} \tag{2d}$$

with p_t and p_a denoting jet total pressure and the ambient pressure, respectively. The Prandtl-Glauert parameter β is thus related to the strength of the normal shock wave. The number of shock reflections for a convergent-divergent nozzle strongly depends on the nozzle design Mach number M_d and the operating pressure ratio.

The relative source strength in each shock-cell can be determined from Eqs. (1) and (2). Eqs. (1a) and (2a) assert that there is successive amplification of the sound waves during their passage through the shock-cell system, with the highest amplification rate occasioned in the first shock-cell. The overall (or total) amplification becomes

$$\frac{\Delta p_m}{\Delta p_{in}} = \left(\frac{\delta p_1}{\delta p_{in}}\right)\left(\frac{\delta p_2}{\delta p_1}\right)\cdots\left(\frac{\delta p_m}{\delta p_{m-1}}\right) \tag{3}$$

where Δp_{in} refers to the disturbance level upstream of the first shock-cell in the vicinity of the nozzle exit.

II. SCREECH CHARACTER

A. Screech Amplitude

The screech amplitude (so-called excess tone level) relative to the broadband spectrum SPL_s is expressed as

$$SPL_s = 20\log_{10}(\Delta p_m / \Delta p_{in}) \tag{4}$$

where $\Delta p_m / \Delta p_{in}$ is determined from Eq. (3). Thus, Eqs. (1a) to (4) enable us to compute the excess (or relative) screech amplitude as a function of jet Mach number. The excess tone noise represents the difference between the screech amplitude and the broadband level (both shock-induced and turbulence-induced) at the screech frequency in a given spectrum (Massey et al. 1993).

The above theory does not display a separate effect of jet temperature on screech tone intensity. Data of Massey et al (1993) suggest that the tone intensity reduces with an increase in temperature. According to the measurements of Massey and Ahuja (1997) mode switching occurs at elevated jet temperature, thereby affecting screech intensity.

B. Screech Directivity

In the present formulation, an extension of Powell's treatment (Powell 1953a, 1953b, 1953c) is considered for the directivity of screech based on stationary point sources along a line (Rayleigh 1888). The farfield radiation is determined synthetically by combining these sources.

With each source of strength of 4π and $4\pi H$ for the fundamental and the first harmonic respectively, the velocity potential distribution for a point source is of the form

$$\phi = \frac{1}{r} e^{ik(ct-r)} + \frac{H}{r} e^{ik(ct-r)} \tag{5}$$

where c denotes the sound speed, r the radial distance, t the time elapsed, and k the wave number, which is related to the wavelength λ of the feedback acoustic wave by

$$\lambda = 2\pi / k \tag{6}$$

Following Powell, we assume that the phases $\tau_1 = \tau_2 = \tau$. For small ratios of s/r (where s denotes the shock-cell spacing), the potential for the fundamental of a three-cell shock system (for example) can be expressed as

$$\phi_f = \frac{(1 + a_2 + a_3)}{r} D_f \cos k(ct - r - \delta_t) \tag{7}$$

The quantities a_2 and a_3 respectively refer to the relative strengths of the second and the third shock-cell with the strength of the first shock-cell taken as unity. The phasing between consecutive monopoles is determined by shock-cell spacing and disturbance convection Mach number M_c (Norum 1982).

The directivity D_f can be expressed as

$$D_f = \frac{1}{(1 + a_2 + a_3)} [a_2 + (1 + a_3) \cos k(c\tau - s \cos\theta)] \tag{8}$$

with

$$\tau = s / u_c = s / (cM_c) \tag{9}$$

where θ denotes the angle from the downstream flow direction and u_c and M_c refer to convective velocity and convective Mach number of the disturbance, respectively. Eq. (8) can be recast as

$$D_f = \frac{1}{(1+a_2+a_3)}\left[a_2 + (1+a_3)\cos\frac{2\pi s}{\lambda M_c}(1 - M_c\cos\theta)\right] \tag{10}$$

Thus, the directionality of screech strongly depends on the shock cell spacing and the disturbance Mach number (Powell 1953a). The quantity $(1 - M_c\cos\theta)$ is a Doppler factor incorporating the variation in retarded time and source phasing (Harper-Bourne & Fisher (1973). An expression for the directivity of the harmonic D_h is provided by Eq. (10) with 2π replaced by 4π. In the special case of $a_2 = a_3 = 1$, Eq. (10) reduces to that derived by Powell (1953a) for uniform source strength. Eq. (10) can be extended to four or more sources.

The shock-cell spacing s is obtained from experimental data and is related to the pressure ratio parameter β defined by

$$s / d_j = f(\beta)$$

For example, data of Harper-Bourne and Fisher (1973) suggest that

$$s / d_j \approx 1.25\beta$$

Experimental data (Powell 1953a) suggest that the shock-cell spacing is related to the feedback acoustic wave length as

$$s / \lambda \approx 0.4 \tag{11}$$

where λ is an integer.

Detailed measurements (Harper-Bourne 2002) suggest that the shock-cell spacing s is not uniform, but varies somewhat along the jet. A non-uniform shock-cell spacing, which may affect the directivity, is unaccounted for in the present theory. Experimental investigations of Massey et al. (1993) also indicate that the effect of heating on the directivity of screech is largely unimportant. No direct effect of jet temperature on the directivity of screech is however evident from Eq. (10).

C. Existing Relations for Screech Frequency

Tam et al. (1986) proposed for the screech frequency a semi-empirical expression of the form

$$fd_j / u_j = f(M_j, \gamma, T_0 / T_a) \tag{12a}$$

where T_a represents the ambient temperature. The fully expanded jet diameter d_j is related to the jet exit diameter and the nozzle design Mach number M_d as

$$d_j / d = f(M_j, M_d, \gamma) \tag{12b}$$

This formula agrees well with the data and accommodates the effect of jet temperature (hot and cold jets). Massey and Ahuja (1997) provided separate expressions, similar in form to Eq. (12), for different screech modes depending on the Mach number range.

The screech frequency increases with temperature since at a fixed Mach number, the convective velocity u_c of the instability wave increases with temperature (Massey et al. 1993). The frequency is inversely proportional to the total time of travel in the screech cycle, $(T_1 + T_2)$, where T_1 refers to the time for the downstream-propagating instability wave to traverse the shock-cell system starting from the nozzle exit, and T_2 the time elapsed for the upstream-propagating feedback acoustic wave to reach the nozzle lip region. Thus, as the temperature increases, the value of T_1 increases so that the frequency decreases.

III. RESULTS AND COMPARISON

In all the results presented here, except for the screech amplitude, all the sound pressure levels (dB) are taken realtive to 20 μ Pa. The quoted levels are in dB linear (unweighted).

A. Streamwise Distribution of Acoustic Source Strength

The streamwise distribution of the acoustic source pressure, as predicted by the present model for the normal shock case, is depicted in Fig. 6 for various Mach numbers. The successive amplification of the stream disturbances along the shock cells is evident, with the source strength increasing with the Mach number. A comparison of the predicted amplification rate with the data of Kaji and Nishijima (1996) for $M_j = 1.64$ and of Panda et al. (1997) for $M_j = 1.19$ and 1.42 is also illustrated here. The data are deduced from the original measurements in order to provide a direct comparison. In this context, it would be instructive to briefly present the data in the original form.

The streamwise amplitude measurements by Kaji and Nishijima (1996) for $M_j = 1.64$ suggest that the highest intensity is located in the shear layer of the third or the fourth shock cell, whereas inside the jet the acoustic intensity is low. Interestingly, the data reveal low-pressure dips (dimple spots) in the source strength. According to Kaji and Nishijima (1996) these dips are believed to be generated by the interaction between sources. There is a possibility that they could also be due to the expansion regions in the flow.

Detailed measurements by Panda et al. (1997) for a circular jet over a wide range of Mach number (M_j = 1.19 to 1.51) show similar trends for the axial distribution of source strength, with the peak values as a whole showing an increasing trend with M_j, ultimately approaching a level of saturation followed by a relatively rapid decline in the screech levels (Fig. 7b).

The foregoing data for the amplification rate are deduced here such that the relative source strength from the data at the first shock cell is taken as that given by the theory. Fig. 6 suggests that the proposed theory for the acoustic source strength $M_j = 1.2$ is in close agreement with the data of Panda et al. (1997) for all the shock cells. However, at Mach numbers of 1.4 and 1.6, the theory overpredicts the amplification rates for downstream shock cells. This discrepancy is perhaps due to the assumption of normal shock.

Numerical simulations by Manning and Lele (2000) for a single shear layer–compression wave interaction suggest that the radiated acoustic pressure amplitude approaches a saturation level at increased distances from the origin of the shear layer (Fig. 7c). The trends of the present model qualitatively agree with these results, although in the exponential region, the amplification rates appear to be comparatively high with respect to those in the present model. However, a direct quantitative comparison of this result with the present model appears difficult in view of the fact that a single compression wave is considered in the computation.

B. Screech Amplitude

Fig. 8 presents the variation of the excess screech amplitude as a function of M_j as provided by the foregoing theory. Experimental data reported by various investigators (including Kaji and Nishijima (1996), Massey and Ahuja (1997) Raman and Rice (1994), Raman (1997), Ponton & Seiner (1992), and Seto et al. (2006) are also displayed here in an effort to validate the physical model. The theory for the normal shock case ($\beta_1 = 90\deg$) suggests that the excess screech amplitude increases from about 17 dB at M_j = 1.05 to about 46 dB at M_j = 2.0, with the slope of the curve slowly diminishing with increasing M_j. The predictions for $\beta_1 = 60\deg$, addressing the sensitivity of the results to the shock wave angle, show about 7 dB reduction in the screech amplitude relative to the normal shock case. The theory seems to be in reasonable agreement with the data from various sources over a range of Mach number, with the normal shock providing the upper limit, and the oblique shock ($\beta_1 = 60\deg$) yielding the lower limit.

Measurements for *absolute* screech amplitude (which includes broadband noise) for a 5:1 aspect ratio rectangular nozzle obtained by Panda et al. (1997) for a wide span of M_j confirm the general character of the present theory (Fig. 9). However, this report does not present the *excess tonal noise* for a direct (quantitative) comparison with the present calculations which provide only the excess screech magnitude. It is believed that the saturation (leveling) of the amplitude at high Mach number (say $M > 4$), as indicated by the data, may be qualitatively explained to some extent if the shock-wave angle varies (decreases) with downstream distance. The relatively rapid decline in the amplitude at $M_j = 1.7$ is perhaps related to the change in the screech mode.

The effect of screech mode on the screech intensity is beyond the scope of the present investigation. The dependence of screech intensity on jet temperature is also excluded from consideration in the present report. A detailed account of nozzle lip thickness is also not addressed here.

C. Screech Directivity

Sample calculations of the directivity of screech for a typical value of M_j = 1.4 for a three-source system are depicted in Figs. 10a and 10b, respectively, for the fundamental and the second harmonic. An effective value of $M_c = 0.7$ is chosen as a representative value. Results for variable strength as obtained from Eq. (10) with $a_2 = 2.75, a_3 = 5.79$ are compared with the case of uniform source strength ($a_2 = a_3 = 1$). The values of a_2 and a_3 are obtained from Fig. 6 at $M_j = 1.4$, relative to the first shock-cell strength of 3.5. For comparison purposes the directivity data of Norum (1983) for a choked nozzle at $M_j = 1.49$ are included. The frequencies of the fundamental and the second harmonic in this data are respectively 19 Hz and 38 Hz.

For the fundamental (Fig. 10a), the directivity pattern displays three lobes. One lobe, namely the principal lobe, radiates upstream and forms part of the feedback loop. The next dominant lobe radiates downstream at a relatively small angle from the downstream flow direction. The third lobe is the weakest one, which radiates in a direction normal to the jet axis. The directivity of the fundamental displaying the predominant lobe in the upstream direction is consistent with the well-known trends of the screech data (Norum 1983). It is evident that the effect of variable strength relative to uniform strength is displayed only in the weakest lobe and is not significant in the primary lobe directed upstream. The data for the fundamental however do not display the weakest lobe (normal to the jet axis).

Fig. 10b for the directivity of the second harmonic suggests that the peak radiation due to screech is in a direction normal to the jet axis—an established result that is in concurrence with the available measurements, such as those of Norum (1983). Again, the variation of strength has some influence on the predicted directionality of the second harmonic in the three subordinate lobes only and does not alter appreciably the directivity of the primary lobe directed normal to the jet axis. The theory considerably underpredicts the upstream lobe levels for the harmonic. Larger number of sources may in general improve the accuracy of the predictions for the directivity- both the fundamental and the second harmonic.

The proposed method is applicable also to a forward flight stream surrounding the jet by appropriately modifying Eq. (2a) and (2b), and with a proper choice for the value of M_c in Eq. (10). Measurements by Krothapalli et al. (1996) with a freestream Mach number from 0 to 0.32 with an underexpanded heated supersonic jet (nozzle pressure ratios up to 4.5) reveal that the screech intensity is unaltered by the forward flight. Cold jet data by Norum and Shearin (1988) indicate the existence of intense screech tones in simulated forward flight up to Mach 0.41.

IV. CONCLUSIONS

Quantitative estimates for the excess screech tone amplitude over a range of fully expanded jet Mach number, as derived from the present model, seem to satisfactorily agree with the experimental data for underexpanded supersonic jets. The predicted streamwise amplification of the acoustic source strength is also found to be consistent with the available measurements, especially at low Mach numbers. This favorable comparison between the theory and the measurements suggests that the proposed physical model for the amplification of downstream-propagating disturbances of finite amplitude based on shock-acoustic wave interaction theory represents a plausible mechanism of screech in the feedback cycle. The results also indicate that the directivity of screech due to variable source strength of the discrete monopole source in each shock-cell does not appreciably differ from that based on uniform source strength insofar as the principal lobes are concerned. The proposed hypothesis for the determination of screech amplitude appears to hold promise in our effort to refine the jet screech modeling.

ACKNOWLEDGMENTS

The author would like to thank the reviewers for valuable suggestions and criticism that considerably improved the manuscript.

REFERENCES

Blokhintsev, D. I., 1945 A moving sound pickup. *Doklady Akad,* Nauk SSSR **47**, 22-25.

Burgers, J. M., 1946 On the transmission of sound waves through a shock wave. *Proc. Ned. Acad. Wet.* **49**, 273-281.

Fisher, M. J. & Morfey, C. L. 1976 Jet Noise. In *AGARD Lecture Series, Aerodynamic Noise,* No. 80.

Fflowcs Williams, J.E., **1963** The noise from turbulence conveccted at high speed, Proc. Roy. Soc. A 255, 469.

Glaznev, V. N., 1973 Some features of the propagation of the discrete tone perturbation in a free supersonic jet. *Fluid Mech. Sov. Res.* **2**, 76-79.

Harper-Bourne, M. & Fisher, M. J. 1973 The noise from shock waves in supersonic jets. In *Proc. AGARD Conference on Noise Mechanisms,* Brussels, Belgium.

Harper-Bourne, M. 2002 On Modeling the near-field noise of the high-speed jet exhausts of combat aircraft, *8th AIAA/CEAS Aeroacosutics Conference*, AIAA-2002-2424, Breckenridge, CO., USA.

Kaji, S. & Nishijima, N., 1996 Pressure field around a rectangular supersonic jet in screech. *AIAA J.* **34**, 1990-1996.

Kandula, M., 2006a An experimental and numerical study of sound propagation from a supersonic jet passing through a rigid-walled duct with a J-deflector, *International Journal of Acoustics and Vibration* **11**, 125-131.

Kandula, M., 2006b Near-field acoustics of clustered rocket engines, accepted for publication in the *Journal of Sound and Vibration*, 2006.

Kandula, M. 2006c A nonlinear shock-refracted acoustic wave model for the prediction of screech amplitude in underexpanded supersonic jets. *12th AIAA/CEAS Aeroacoustics Conference*, AIAA-2006-2674, Boston, Massachusetts, USA.

Kontorovich, V. M., 1960 Reflection and refraction of sound by shock waves. *Soviet Physics – Acoustics* **5**, 320-330.

Krothapalli, A., Hsia, Y., Baganoff, D. & Karamcheti, K. 1986 The role of screech tones in mixing of underexpanded rectangular jet. *J. Sound and Vibration* **116**,119-143.

Li, X. D. & Gao, J. H. 2005 Numerical simulation of three-dimensional supersonic jet screech tones. *11th AIAA/CEAS Aeroacoustics Conference,* AIAA-2005-2882, Monterey, CA, USA.

Li, X. D. & Gao, J. H. 2004 Numerical simulation of three-dimensional supersonic screech tones. *10th AIAA/CEAS Aeroacoustics Conference,* AIAA-2004-2951, Manchester, England.

Lighthill, M.J., 1954 On sound generated aerodynamically, I. General theory, Proc. Roy. Soc. A **211**, 564-587.

Lighthill, M.J., 1952 On sound generated aerodynamically, II. Turbulence as a source of sound, Proc. Roy. Soc. A **222**, 1-32.

Loh, C. Y., Himansu, A & Hultgren, L. S. 2003 A 3-D CE/SE Navier-Stokes solver with unstructured hexahedral grid for computation of near field jet screech noise. *9th AIAA/CEAS Aeroacoustics Conference,* AIAA-2003-3207, Hilton Head, South Carolina, USA.

Lui, C., and Lele, S. K. 2002 A numerical study of shock-associated noise. *8th AIAA/CEAS Aeroacoustics Conference,* AIAA-2002-2530, AIAA, Breckenridge, Colorado, USA.

Manning, T. A. & Lele, S. K. 1998 Numerical simulations of shock vortex interactions in supersonic jet screech. AIAA-98-0282.

Manning, T. A. & Lele, S. K. 2000 A numerical investigation of sound generation in supersonic jet screech. AIAA-2000-2081.

Massey, K. C., Ahuja, K. K., Jones, III, R. R.& Tam, C. K. W. 1993 Screech tones of supersonic heated free jets. *32nd Aerospace Sciences Meeting,* AIAA-93-0141, Reno, Nevada, USA.

Massey, K. C. & Ahuja, K. K. 1997 Screech frequency prediction in light of mode detection and convection speed measurements for heated jets. AIAA-97-1625.

McKenzie, J. F. & Westphal, K. O. 1968 Interaction of linear waves with oblique shock waves. *Phys. of Fluids* **11**, 2350-2362.

Norum, T. D. 1983 Screech suppression in supersonic jets. *AIAA J.* 21, 235-240.

Norum, T. & Shearin, J.G., 1988 Shock sturcture and noise of supersonic jets in simulated flight to Mach 0.4, NASA TP 2785.

Panda, J., Raman, G. & Zaman, K. 1997 Underexpanded screeching jets from circular, rectangular and elliptic nozzles. *3rd AIAA/CEAS Aeroacoustics Conference,* AIAA-97-1623.

Panda, J., 1998 Shock oscillation in underexpanded jets. *J. Fluid Mech.* **363**, 173-198.

Panda, J. 1999 An experimental investigation of screech noise generation. *J. Fluid Mech.* **378**, 71-96.

Panda, J. 1996 An experimental investigation of screech noise generation. AIAA-96-1718.

Petitjean, B. P., Morris, P. J. & McLaughlin, D. K. 2005 On the nonlinear propagation of shock-associated noise. *11th AIAA/CEAS Aeroacoustics Conference,* AIAA-2005-2930, Monterey, California, USA.

Ponton, M.K. & Seiner, J.M. 1992 The effects of nozzle lip thickness on plume resonance. *J. Sound and Vibration* **154**, 531-549.

Powell, A. 1953 On the mechanism of choked jet noise. *Proc. Phys. Soc. London B* **4**, 1039-1056.

Powell, A. 1953 On the noise emanating form a two-dimensional jet above the critical pressure. *The Aeronautical Quarterly* **4**, 103-122.

Powell, A., The noise of choked jets. *J. Acoustical Soc. Amer.* **25**, 385-389.

Raman, G. 1998 Advances in understanding supersonic jet screech: Review and Perspective. *Progr. Aerospace Sciences* **34**, 45-106.

Raman, G. 1999 Supersonic jet screech: Half-century from Powell to the present. *J. Sound and Vibration* **225**, 543-571.

Raman, G. & Rice, E.J., Instability modes excited by natural screech tones in a supersonic rectangular jet. *Phys. of Fluids* **6**, 3994-4008.

Raman, G. 1997 Cessation of screech in underexpanded jets. *J. Fluid Mech.* **336**, 69-90.

Rayleigh, Lord, 1888 On point-, line- and plane-sources of sound," *Proc. London Math. Soc.* **19**, 504.

Sedel'nikov, T. Kh. 1967 The discrete component of the frequency spectrum of the noise of a free supersonic jet. In *Physics of Aerodynamic Noise (ed.* A. V. Rimskiy-Korsakov), Nauka, Moscow.

Seiner, J.M. 1984 Advances in high speed jet aeroacoustics. AIAA-84c-2275, *AIAA/NASA 9th Aeroacoustics Conference*, Williamsburg, Virginia.

Seto, K., Khan, M.T.I. & Teramoto, K. 2006 The reduction of jet noise with spherical reflector and evaluation of its performance compared to a flat reflector, *Int. J. Acoustics & Vibration*, **11**, 187-195.

Shapiro, A. H. 1953 *The Dynamics and Thermodynamics of Compressible Fluid Flow,* Vol. 1, Wiley, New York.

Shen, S. & Tam, C. K. W. 1998 Numerical simulation of the generation of axisymmetric mode jet screech tones. *AIAA J.* **36**, 1801-1807.

Shen, H. & Tam, C. K. W 2002 Three-dimensional numerical simulation of the jet screech phenomenon. *AIAA J.* **40**, 33-41.

Tam, C. K. W., Seiner, J. M. & Yu, J. C. 1986 Proposed relationship between broadband shock associated noise and screech tones. *J. Sound and Vibration* **110**, 309-321.

Tam, C. K. W. 1987 Stochastic model theory of broadband shock associated noise from supersonic jets. *J. Sound and Vibration* **116**, 265-302.

Zong, T.A., Hussain, M.Y., and Bushnell, D.M. 1984 Numerical computation of turbulence amplification in shock-wave interactions, *AIAA J.*, **22**, 13-21.

Captions to Figures

FIG. 1. A typical narrowband farfield shock noise spectrum (adapted from Seiner 1984).

FIG. 2. Schematic of the feedback loop in supersonic jet screech according to Powell (1953a).

FIG. 3. Idealized distribution of acoustic sources in an underexpanded jet.

FIG. 4. Interaction of an acoustic wave with a stationary shock wave (McKenzie & Westphal 1958).

FIG. 5. Acoustic pressure amplification as a function of upstream Mach number.

FIG. 6. Streamwise amplification of acoustic source strength from present theory.

FIG. 7a. Streamwise amplification of acoustic source strength from the data of Kaji & Nishijima (1996) for $M_j = 1.64$.

FIG. 7b. Streamwise amplification of acoustic source strength from the data of Panda (1997).

FIG. 7c. Streamwise amplification of acoustic source strength from the numerical simulation of Manning & Lele (2000).

FIG. 8. Comparison of the dependence of excess screech amplitude on Mach number.

FIG. 9. Dependence of measured screech amplitude on Mach number, from data of Panda (1997).

FIG. 10a. Directivity of the screech fundamental.

FIG. 10b. Directivity of screech second harmonic.

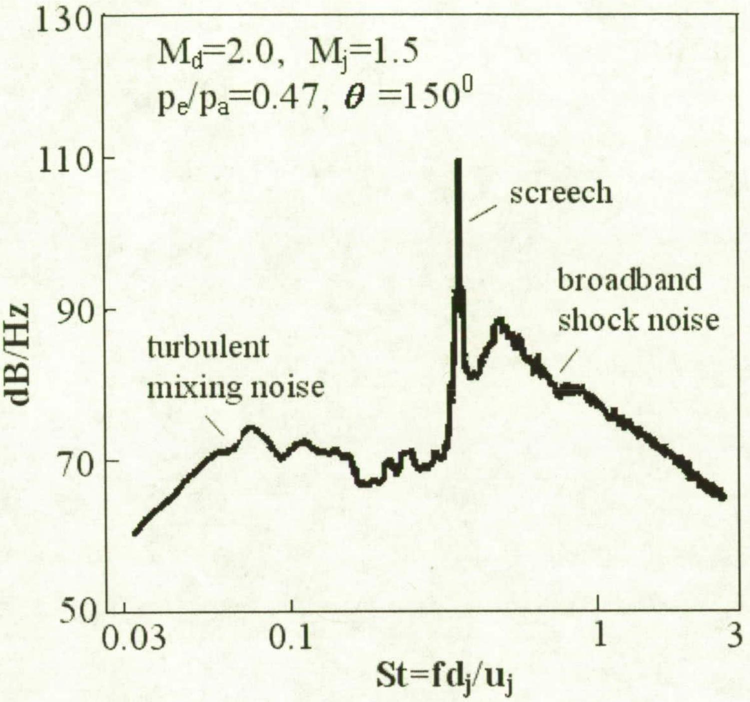

FIG. 1. A typical narrowband farfield shock noise spectrum (adapted from Seiner 1984).

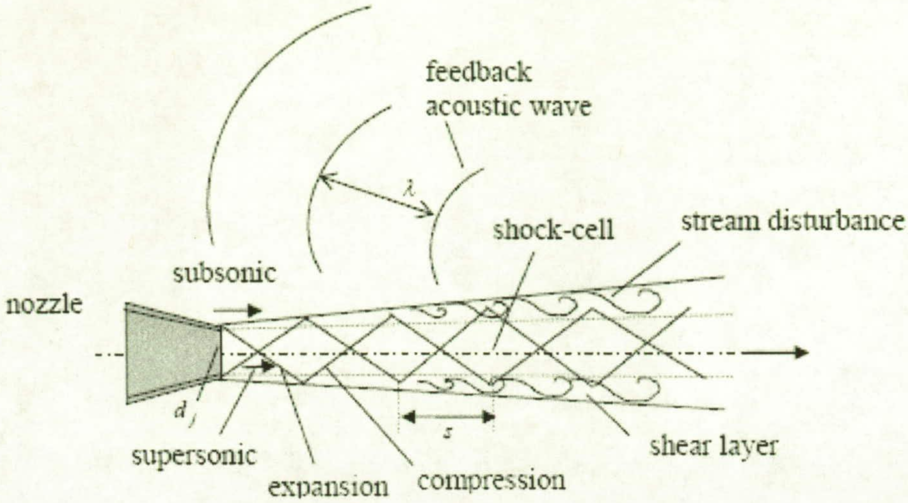

FIG. 2. Schematic of the feedback loop in supersonic jet screech according to Powell (1953a-c)

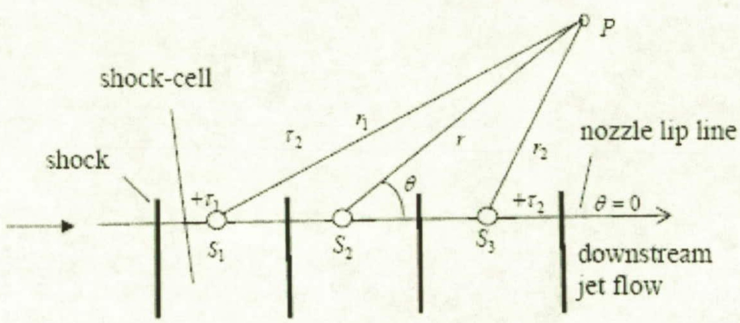

FIG. 3. Idealized distribution of acoustic sources in an underexpanded jet.

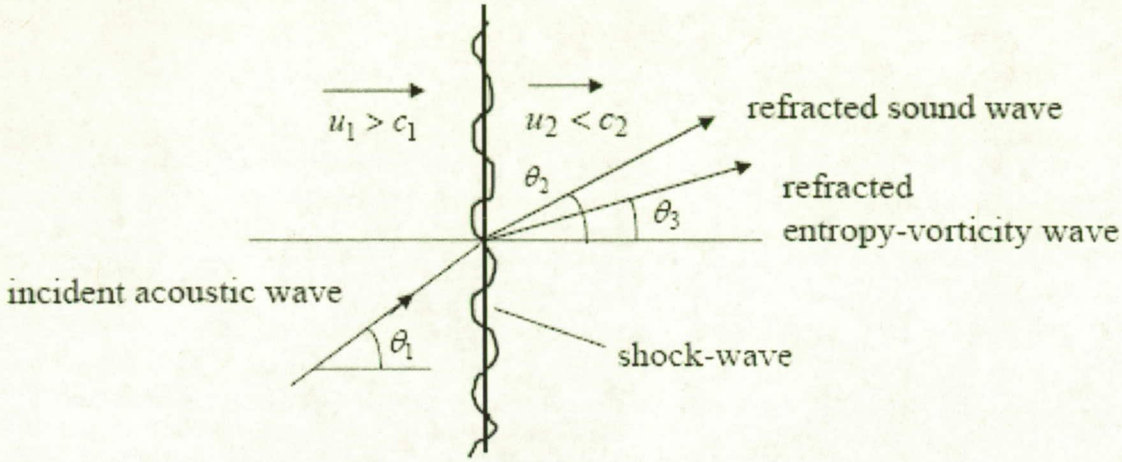

FIG. 4. Interaction of an acoustic wave with a stationary shock wave (McKenzie and Westphal 1958).

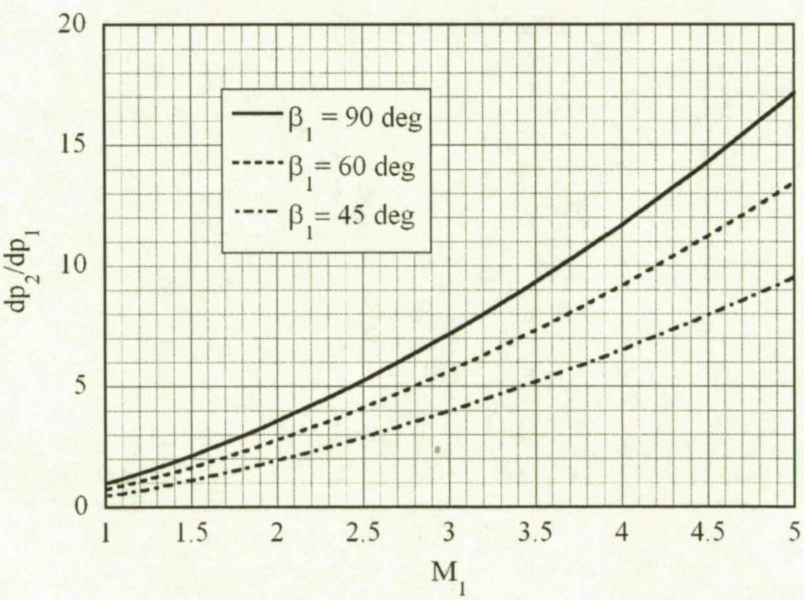

FIG. 5. Acoustic pressure amplification as a function of upstream Mach number.

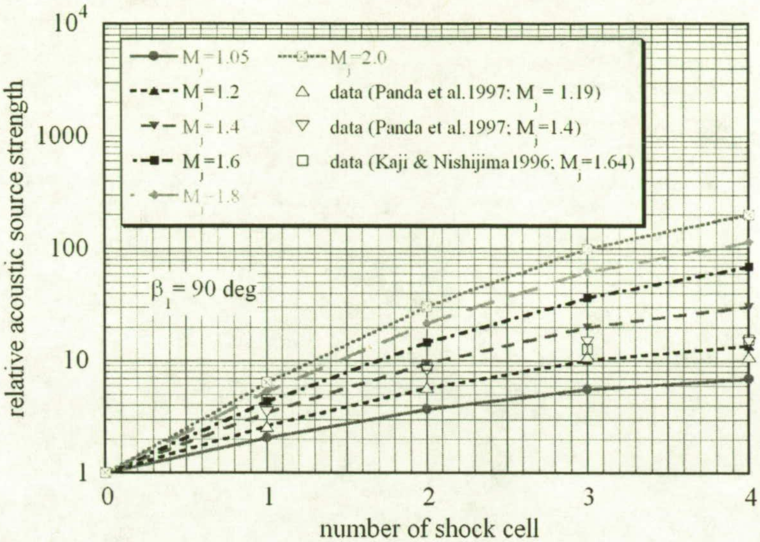

FIG. 6. Streamwise amplification of acoustic-source strength from present theory.

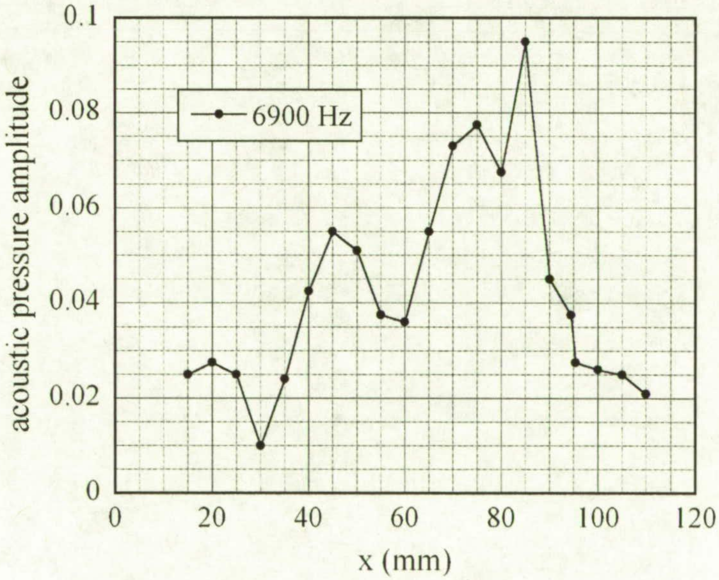

FIG. 7a. Streamwise amplification of acoustic source strength from the data of Kaji and Nishijima for $M_j = 1.64$.

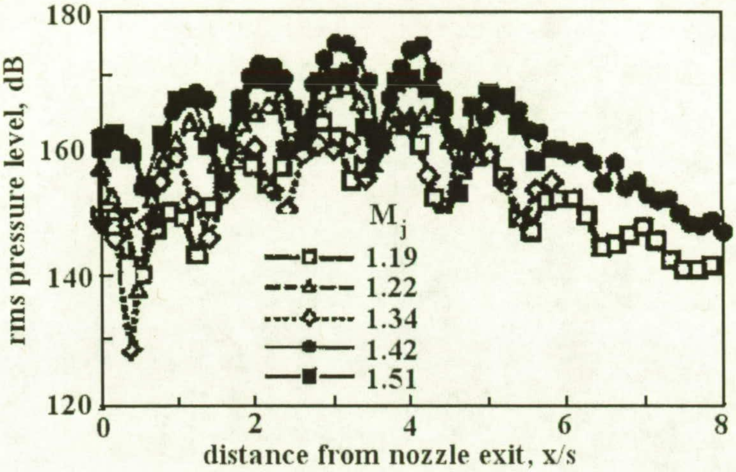

FIG. 7b. Streamwise amplification of acoustic-source strength from the data of Panda (1997).

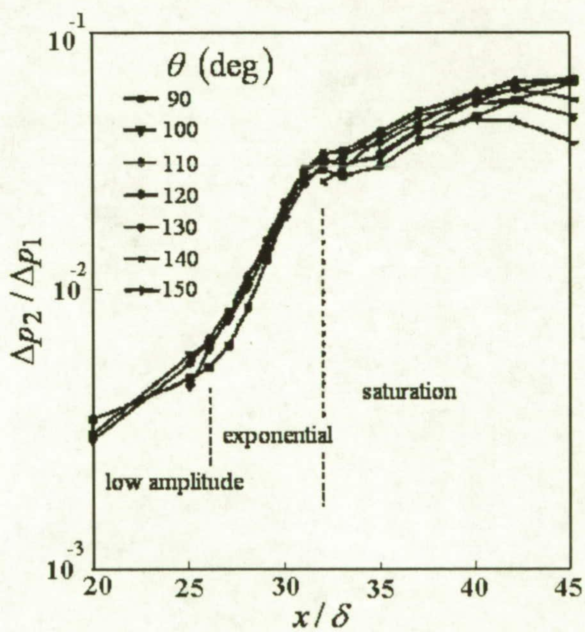

FIG. 7c. Streamwise amplification of acoustic-source strength from the numerical simulation of Manning and Lele (2000).

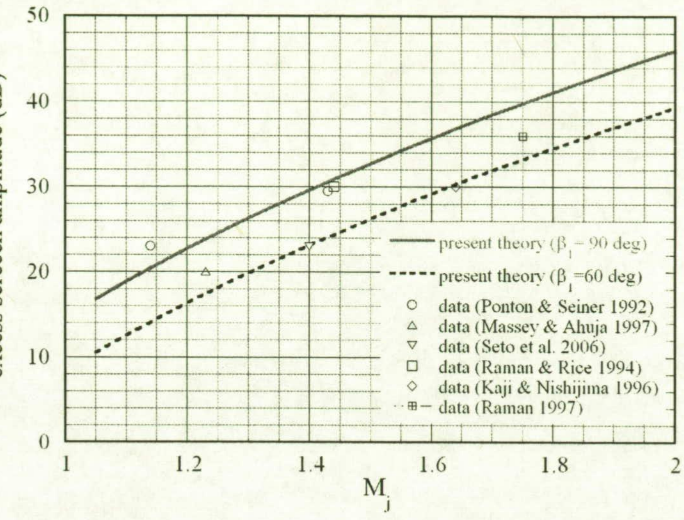

FIG. 8. Comparison of the dependence of excess screech amplitude on Mach number.

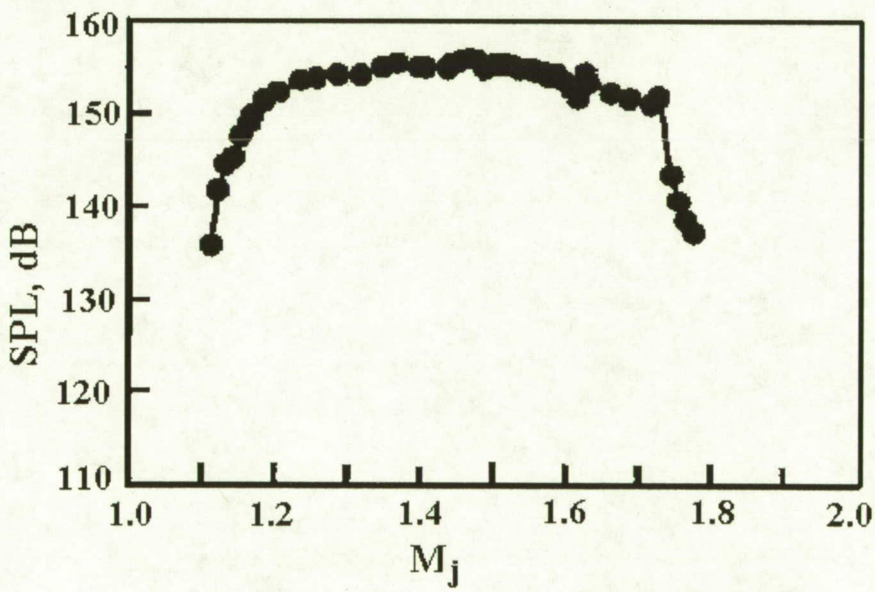

FIG. 9. Dependence of measured screech amplitude on Mach number, from data of Panda (1997).

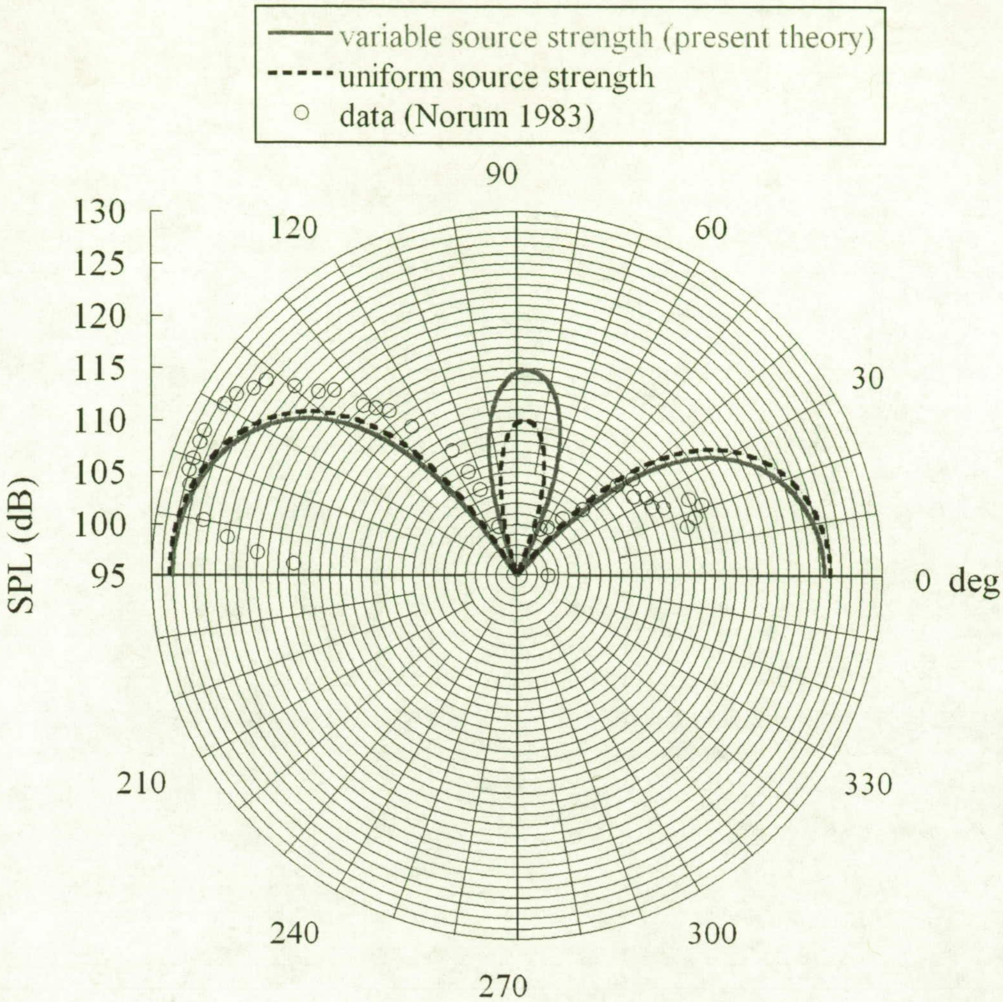

FIG. 10a. Directivity of the screech fundamental.

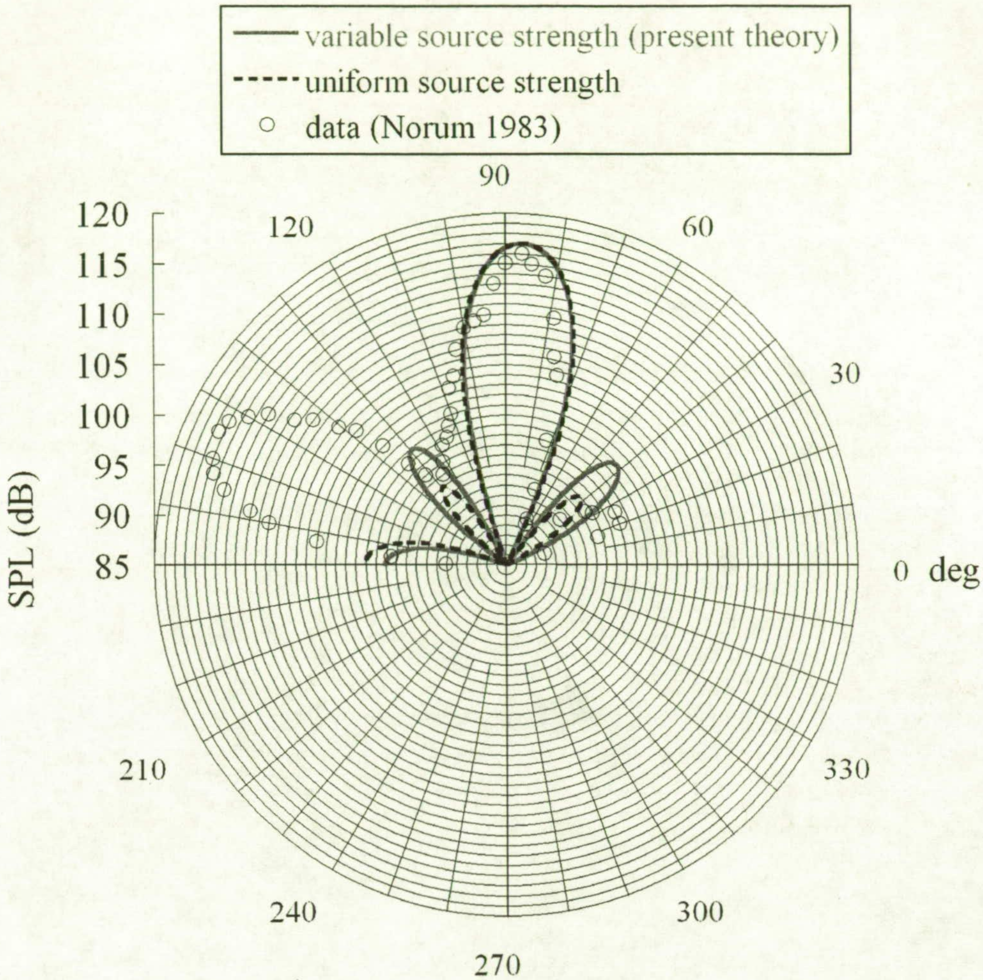

FIG. 10b. Directivity of the screech second harmonic.